The Human K-Complex Represents an Isolated Cortical Down-State

Sydney S. Cash, *et al.*

Science **324**, 1084 (2009);
DOI: 10.1126/science.1169626

ficed to establish place preference in the absence of other reward. These results establish a causal role in behavioral conditioning for defined spiking modes in a specific cell type; of course, even a single cell type can release multiple neurotransmitters and neuromodulators (for example, VTA DA neurons primarily release DA but can also release other neurotransmitters such as glutamate) and will exert effects through multiple distinct downstream cell types. Indeed, the optogenetic approach, integrated with electrophysiological, behavioral, and electrochemical readout methods, opens the door to exploring the causal, temporally precise, and behaviorally relevant interactions of DA neurons with other neuromodulatory circuits (*22*–*25*), including monoaminergic and opioid circuits important in neuropsychiatric illnesses (*26*–*28*). In the process of identifying candidate interacting neurotransmitter systems, downstream neural circuit effectors (*29*), and subcellular biochemical mechanisms on time scales appropriate to behavior and relevant circuit dynamics, it will be important to continue to leverage the specificity and temporal precision of optogenetic control (*30*).

References and Notes

1. R. A. Wise, *Nat. Rev. Neurosci.* **5**, 483 (2004).
2. B. J. Everitt, T. W. Robbins, *Nat. Neurosci.* **8**, 1481 (2005).
3. T. E. Robinson, K. C. Berridge, *Brain Res. Brain Res. Rev.* **18**, 247 (1993).
4. G. F. Koob, M. Le Moal, *Science* **278**, 52 (1997).
5. W. Schultz, *Annu. Rev. Neurosci.* **30**, 259 (2007).
6. M. A. Ungless, P. J. Magill, J. P. Bolam, *Science* **303**, 2040 (2004).
7. F. Zhang, Larry C. Katz Memorial Lecture presented at the Cold Spring Harbor Laboratory Meeting on Neuronal Circuits, Cold Spring Harbor, NY, 13 to 16 March 2008.
8. D. Atasoy, Y. Aponte, H. H. Su, S. M. Sternson, *J. Neurosci.* **28**, 7025 (2008).
9. E. S. Boyden, F. Zhang, E. Bamberg, G. Nagel, K. Deisseroth, *Nat. Neurosci.* **8**, 1263 (2005).
10. G. Nagel *et al.*, *Proc. Natl. Acad. Sci. U.S.A.* **100**, 13940 (2003).
11. Materials and methods are available as supporting material on *Science* Online.
12. A. Bjorklund, S. B. Dunnett, *Trends Neurosci.* **30**, 194 (2007).
13. Q. S. Liu, L. Pu, M. M. Poo, *Nature* **437**, 1027 (2005).
14. S. Robinson, D. M. Smith, S. J. Mizumori, R. D. Palmiter, *Proc. Natl. Acad. Sci. U.S.A.* **101**, 13329 (2004).
15. A. R. Adamantidis, F. Zhang, A. M. Aravanis, K. Deisseroth, L. de Lecea, *Nature* **450**, 420 (2007).
16. P. E. Phillips, G. D. Stuber, M. L. Heien, R. M. Wightman, R. M. Carelli, *Nature* **422**, 614 (2003).
17. G. D. Stuber *et al.*, *Science* **321**, 1690 (2008).
18. T. M. Tzschentke, *Addict. Biol.* **12**, 227 (2007).
19. C. M. Cannon, R. D. Palmiter, *J. Neurosci.* **23**, 10827 (2003).
20. A. A. Grace, S. B. Floresco, Y. Goto, D. J. Lodge, *Trends Neurosci.* **30**, 220 (2007).
21. T. S. Hnasko, B. N. Sotak, R. D. Palmiter, *J. Neurosci.* **27**, 12484 (2007).
22. P. W. Kalivas, *Am. J. Addict.* **16**, 71 (2007).
23. M. R. Picciotto, W. A. Corrigall, *J. Neurosci.* **22**, 3338 (2002).
24. J. A. Dani, D. Bertrand, *Annu. Rev. Pharmacol. Toxicol.* **47**, 699 (2007).
25. G. C. Harris, G. Aston-Jones, *Neuropsychopharmacology* **28**, 865 (2003).
26. E. J. Nestler, W. A. Carlezon Jr., *Biol. Psychiatry* **59**, 1151 (2006).
27. J. Williams, P. Dayan, *J. Child Adolesc. Psychopharmacol.* **15**, 160 (2005).
28. A. M. Graybiel, *Annu. Rev. Neurosci.* **31**, 359 (2008).
29. W. Shen, M. Flajolet, P. Greengard, D. J. Surmeier, *Science* **321**, 848 (2008).
30. F. Zhang *et al.*, *Nature* **446**, 633 (2007).

31. We thank M. Wightman, P. Phillips, and the entire Deisseroth laboratory for their support. All reagents and protocols are freely distributed and supported by the authors (www.optogenetics.org); because these tools are not protected by patents, Stanford University has applied for a patent to ensure perpetual free distribution to the international academic nonprofit community. H.C.T. is supported by a Stanford Graduate Fellowship. F.Z. and G.D.S. are supported by NIH National Research Service award. A.R.A. is supported by the Fonds National de la Recherche Scientifique, NARSAD, and the Fondation Leon Fredericq. L.d.L. is supported by National Institute on Drug Abuse (NIDA), Defense Advanced Research Projects Agency, and NARSAD. K.D. is supported by NSF; National Institute of Mental Health; NIDA; and the McKnight, Coulter, Snyder, Albert Yu and Mary Bechmann, and Keck foundations.

Supporting Online Material

www.sciencemag.org/cgi/content/full/1168878/DC1
Materials and Methods
Figs. S1 to S7
References

24 November 2008; accepted 7 April 2009
Published online 23 April 2009;
10.1126/science.1168878
Include this information when citing this paper.

The Human K-Complex Represents an Isolated Cortical Down-State

Sydney S. Cash,[1]*† Eric Halgren,[2]* Nima Dehghani,[2] Andrea O. Rossetti,[5] Thomas Thesen,[3] ChunMao Wang,[3] Orrin Devinsky,[3] Ruben Kuzniecky,[3] Werner Doyle,[3] Joseph R. Madsen,[4] Edward Bromfield,[5] Loránd Erőss,[6] Péter Halász,[7,9] George Karmos,[8,9] Richárd Csercsa,[8] Lucia Wittner,[6,8] István Ulbert[6,8,9]*

The electroencephalogram (EEG) is a mainstay of clinical neurology and is tightly correlated with brain function, but the specific currents generating human EEG elements remain poorly specified because of a lack of microphysiological recordings. The largest event in healthy human EEGs is the K-complex (KC), which occurs in slow-wave sleep. Here, we show that KCs are generated in widespread cortical areas by outward dendritic currents in the middle and upper cortical layers, accompanied by decreased broadband EEG power and decreased neuronal firing, which demonstrate a steep decline in network activity. Thus, KCs are isolated "down-states," a fundamental cortico-thalamic processing mode already characterized in animals. This correspondence is compatible with proposed contributions of the KC to sleep preservation and memory consolidation.

Although the electroencephalogram (EEG) is known to directly and instantaneously reflect synaptic and active transmembrane neuronal currents, the specific channels, synapses, and circuits that generate particular EEG elements in humans remain poorly specified. Much of the EEG is composed of repeated wave forms with characteristic morphologies, durations, amplitudes, frequency content, evoking events, and background states (*1*). The largest of these EEG "graphoelements" is the KC, characterized by a short surface-positive transient followed by a slower, larger surface-negative complex with peaks at 350 and 550 ms, and then a final positivity peaking near 900 ms, followed sometimes by 10- to 14-Hz "spindles" (*2*–*4*). KCs occur in non–rapid-eye-movement (non-REM) sleep, especially stage 2. Deeper sleep (stages 3 to 4) is characterized by slow waves, demonstrated in extensive animal studies to consist of a "slow oscillation" between periods of intense firing by both excitatory and inhibitory cortical neurons (termed "up-states") and periods of neuronal silence ("down-states") (*5*–*9*). Using micro- and macro-electrode arrays placed in patients undergoing evaluation for epilepsy (*10*), we demonstrate that the microphysiological characteristics of human KCs appear identical to those of down-states recorded in the same patients.

Typical KCs were recorded in eight patients (*11*). KCs were either spontaneous or evoked by a weak auditory stimulus. Within a given patient, the basic KC wave forms were similar regardless of whether they were recorded at the scalp or intracranially (Fig. 1A). In all cases, the wave form was dominated by a large deflection occurring ~500 to 600 ms after the onset of a stimulus, or after the onset of the initial deflection for spontaneous KCs. Characteristic KC wave forms were recorded by subdural electrodes placed on all cortical lobes, demonstrating widespread

[1]Department of Neurology, Epilepsy Division, Massachusetts General Hospital, Harvard Medical School, Boston, MA 02114, USA. [2]Departments of Radiology, Neurosciences, and Psychiatry, University of California at San Diego, San Diego, CA 92093, USA. [3]Comprehensive Epilepsy Center, New York University School of Medicine, New York, NY 10016, USA. [4]The Children's Hospital, Boston, MA 02115, USA. [5]Brigham and Women's Hospital, Boston, MA 02115, USA. [6]National Institute of Neurosurgery, H-1145 Budapest, Hungary. [7]National Institute of Psychiatry and Neurology, Epilepsy Center, H-1145 Budapest, Hungary. [8]Institute for Psychology, Hungarian Academy of Sciences, H-1394 Budapest, Hungary. [9]Péter Pázmány Catholic University, Department of Information Technology, H-1083 Budapest, Hungary.

*These authors contributed equally to this work.
†To whom correspondence should be addressed. E-mail: scash@partners.org

generation (Fig. 1B). In all scalp and most intracranial sites, this deflection was surface-negative. Different KCs recorded in the same patient varied in their relative size and timing across cortical locations (Fig. 1C). That is, KCs were not completely synchronous across the cortical surface, nor were the direction or duration of the transcortical delays constant across different KCs.

Potential gradients across cortical layers during KCs were recorded during these same events by using linear arrays of microelectrodes in temporal, frontal, and parietal sites (Fig. 1A). In all cases, KCs seen on the scalp electrodes were also observed on microelectrodes of the array and vice versa. Spontaneous and evoked KCs were recorded in four patients. They showed similar wave-form characteristics and distribution (Figs. 1D and 2), with the maximal negative response present on the same recording channel. No significant differences were found in the peak amplitude or area under the curve during this peak between spontaneous and evoked KCs (*t* test and Kolmogorov-Smirnov test; powered ≥0.80 to detect a 20% difference at $P < 0.05$).

Current source density calculated from these data showed a consistent pattern for both spontaneously occurring and triggered KCs. During the surface-negative slow deflection, there was a current sink in the channels closest to the cortical surface, whereas a substantial source was present in middle channels ~450 to 600 μm below the sink. This pattern, observed in all subjects, likely corresponds to a passive sink centered in layer I and an active source centered in layer III (Figs. 2, A and B, and 3A1). Successful recordings of multiunit neuronal firing were obtained in four subjects, all of whom showed decreased firing during the surface-negative slow deflection of either spontaneous or evoked KCs (Figs. 2, A and B, and 3A2). The pattern of sinks and sources and the decreased neuronal firing changes described here indicate hyperpolarizing current flow in layer III during the large surface-negative deflection.

Analysis of the spectral content of both spontaneous and evoked events consistently demonstrated a broadband decrease in the activity during the surface-negative event in multiple cortical layers when we used microelectrodes and in multiple locations with subdural macroelectrodes (Fig. 3). This was particularly pronounced for higher-frequency (gamma) activity from 20 to 100 Hz; low-frequency components—representing the wave form itself—were often maintained. High frequencies could remain depressed past resolution of the negative deflection. In six subjects, higher-frequency power briefly increased at KC onset. However, in no case was the surface-negative slow event preceded by rhythmic modulations of current or gamma power.

This study provides strong evidence that KCs are induced cortical down-states. First, our recordings demonstrate that KCs are generated in widespread cortical locations. Previous extracranial EEG (*12*), magnetoencephalogram (MEG) (*13*), and intracranial EEG recordings (*14*, *15*) have not provided unambiguous localization of KC generators because of difficulties in localizing widely distributed sources. Local KC generation near the electrode contact is highly likely in our recordings from the cortical surface and is certain when steep gradients are recorded at 150-μm intervals with microelectrode arrays. Widespread intracortical generation of KCs is consistent with the generation of down-states in lower mammals, which arise in distributed cortico-cortical networks (*16*).

The current study also demonstrates that KCs in humans are associated with strong and consistent decreases in gamma and multiunit activity, similar to those observed in animals during the down-state and indicating widespread decreases in cortical activity (*5*, *6*, *8*, *9*, *17*). Direct confirmation of identical microphysiology was obtained in our subjects by comparing KC and slow-oscillation down-states recorded within the same sleep session and by the same microelectrode arrays (Fig. 2). Even at the 150-μm resolution of these recordings, the two conditions evoke identical laminar distributions of transmembrane currents (correlation coefficient at the peak of the deflection was 0.95 between spontaneous KC and slow waves and 0.96 between evoked KC and slow waves, with $P < 10^{-12}$ for both). The indices of network synaptic activity (gamma power) and of population firing (multiunit activity) were both decreased during the KC in all cortical layers, but especially in the supragranular layers, as is characteristic of the slow-oscillation down-state (Fig. 3). Finally, although various inhibitory processes in the cortex have a wide range of durations, from less than 20 ms to several seconds, the KC and slow-oscillation down-states both last ~400 ms.

Although the data thus strongly support the proposal of Amzica and Steriade (*7*) that the KC reflects a cortical down-state, it does not support their corollary proposal that the KC is always part of an underlying oscillation (*18*). Rather, our evidence indicates that, at both the intracortical and epicortical levels, isolated KCs are the rule rather than the exception during stage 2 sleep. This is consistent with numerous observations over the past 70 years (*2*–*4*). Also consistent with these previous studies, but in contrast with Amzica and Steriade (*7*), we found the major component of KCs to be surface-negative.

The down-state is characterized by hyperpolarizing potassium currents, as well as low synaptic activity (*6*). The lack of a local up-state preceding the KC may pose difficulties for the proposal that an activity-dependent accumulation of calcium or adenosine diphosphate (ADP) triggers a potassium current and, thus, the down-state (*19*–*21*). Our findings, as well as recent evidence that the onset of the down-state is more synchronous than that of the up-state (*16*), suggest the need for additional synchronizing mecha-

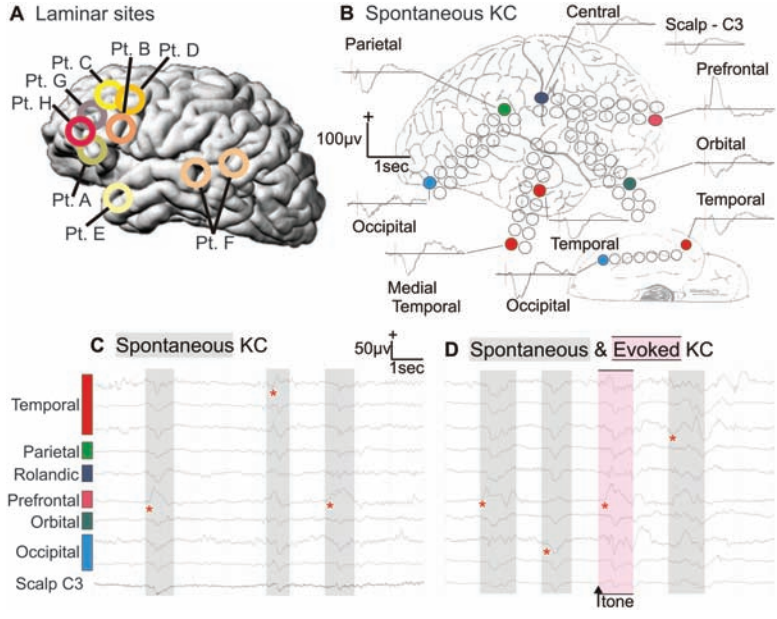

Fig. 1. Spontaneous and evoked KCs recorded simultaneously from the surface of all cortical lobes. (**A**) Approximate locations of microelectrode arrays in the eight patients (Pt.) studied. (**B**) Averaged spontaneous KCs recorded with grid electrodes in multiple cortical locations and from the scalp (subject E). Unaveraged spontaneous (**C** and **D**) and evoked (D) KCs from the same electrodes. Red asterisks show earliest deflection during the KCs and demonstrate the variability in onset and spread. Sleep stages and KCs were identified during natural sleep with standard criteria (*27*). KCs were evoked with occasional tones. Subdural electrode arrays were placed to confirm the hypothesized seizure focus and to locate epileptogenic tissue in relation to essential cortex, so as to direct surgical treatment.

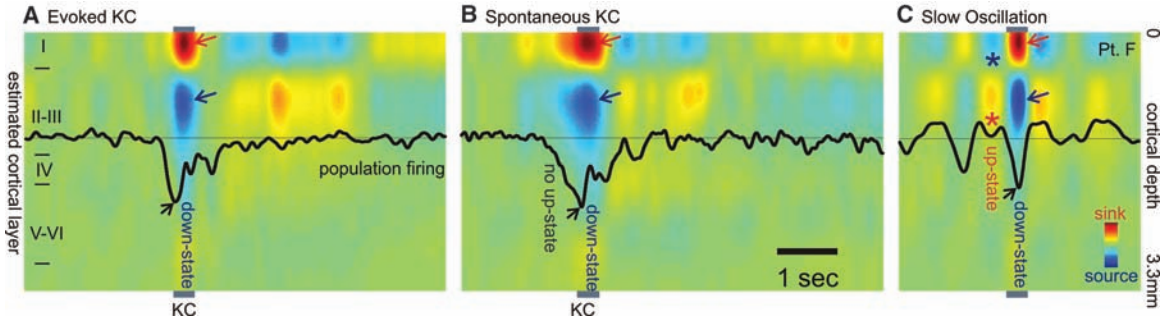

Fig. 2. Population transmembrane currents and neuronal firing in different cortical layers during single evoked (**A**) and spontaneous (**B**) KC in stage 2 sleep, and (**C**) during the slow oscillation in stage 3 to 4 sleep. Evoked and spontaneous KC and the slow-oscillation down-state are all characterized by outward currents (sources) in cortical layers II to III (blue arrows), paired with inward currents (sinks) near the cortical surface (red arrows), and decreased neuronal firing (black arrows). Unlike the KC, the slow-oscillation down-state is embedded in rhythmic alternation with up-states consisting of layer II/III sinks (*), layer I sources (*), and increased firing. Patient F.

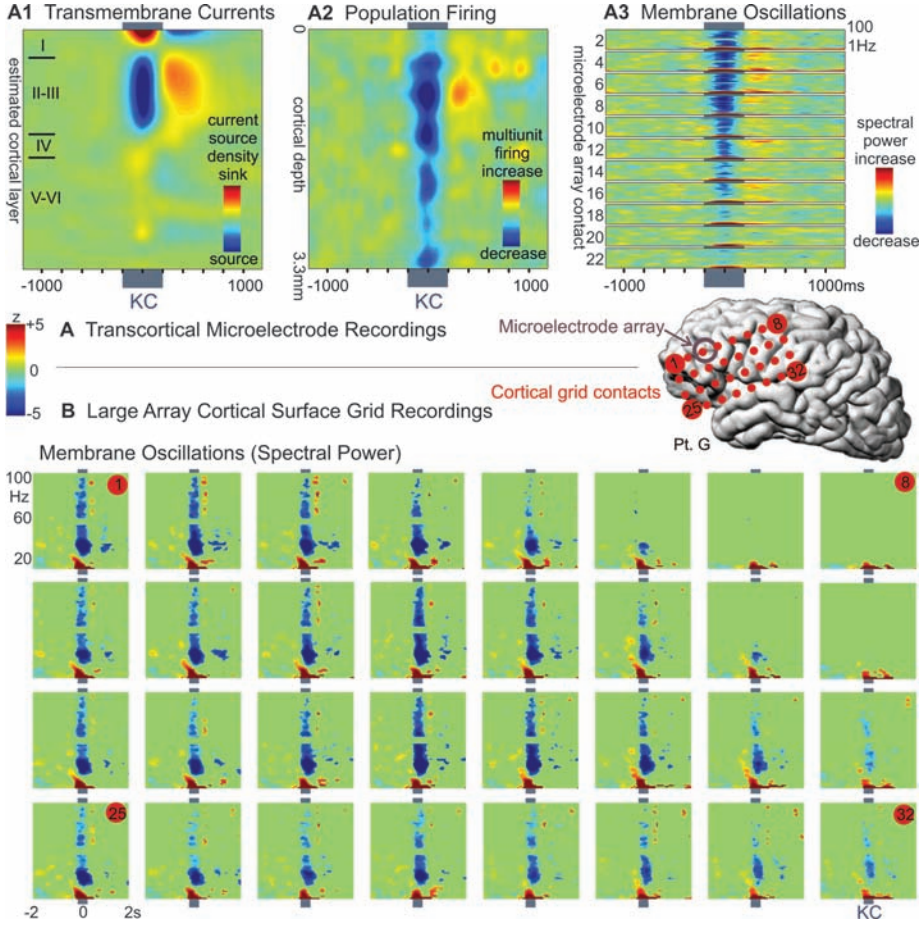

Fig. 3. Decrement in population firing and high-frequency membrane oscillations during KC. (**A**) Microelectrode array recordings of (A1) averaged spontaneous KCs show a layer III source, (A2) decreased neuronal firing, and (A3) membrane oscillations (higher-frequency spectral power), in all layers, especially upper layers. (**B**) Simultaneous recordings in the same patient from a large grid array of electrodes on the cortical surface also show a decrease in high-frequency spectral power during KC. Plots are set to the same threshold to show significant ($P < 0.01$) spectral power changes compared with a period of 1500 to 250 ms before the KC.

nisms, for instance, cortico-thalamo-cortical interactions, as have been shown for the sleep spindle (*22*). For example, in the tone-evoked KC, initial medial geniculate and auditory cortex activation could trigger a local down-state that spreads via thalamo-cortical and cortico-cortical connections. KCs would then occur spontaneously because of a similar mechanism, only with the sensory stimulus occult to the investigator (e.g., gastric), or because of a spontaneous burst of cortical activity. Thus, the KC down-state may follow an up-state, but only in the initiating zone. Our finding that successive KCs arise in variable cortical locations (Fig. 1D), which confirmed scalp recordings (*12*) and computational models (*19*), is consistent with this interpretation.

Sleep is thought to perform essential restorative and mnestic functions (*23*). Maintaining sleep is therefore crucial, but so is awakening in the face of danger. Our finding that the KC represents an isolated down-state supports the theory that it suppresses cortical activity and, thus, arousal in response to stimuli that are judged by the sleeping brain not to be dangerous (*3*, *4*). Increasing evidence supports a strong contribution to memory consolidation of stage 2 sleep, characterized by KC and spindles (*24*). The cortical down-state may provide a period when the near absence of neural activity induces a blanket suppression of synaptic strengths, balancing the synaptic enhancement occurring during waking and up-states and thus preserving the signal-to-noise ratio in network representations (*25*). In addition, during the recovery from the down-state, cortical firing "reboots" in a systematic order, which allows the potential for engrams encoded in dynamic assemblies of neuronal firing to be repeatedly practiced and thus consolidated (*26*). The current study ties a universal, normal, prominent, easily-observed EEG phenomenon to its underlying substrate of membrane currents and neuronal circuits through direct observation and homology with animal studies. This allows previous observations relating human sleep EEG to memory and sensory arousal to be interpreted within mechanistic neural models.

References and Notes

1. G. Buzsaki, *Rhythms of the Brain* (Oxford Univ. Press, Oxford, 2006).
2. A. L. Loomis, E. N. Harvey, G. Hobart, *J. Neurophysiol.* **13** (suppl.), 231 (1938).
3. I. M. Colrain, *Sleep* **28**, 255 (2005).
4. P. Halasz, *Sleep Med. Rev.* **9**, 391 (2005).
5. M. Steriade, F. Amzica, A. Nunez, *J. Neurophysiol.* **70**, 1385 (1993).
6. D. Contreras, I. Timofeev, M. Steriade, *J. Physiol.* **494**, 251 (1996).
7. F. Amzica, M. Steriade, *Neuroscience* **82**, 671 (1998).
8. M. V. Sanchez-Vives, D. A. McCormick, *Nat. Neurosci.* **3**, 1027 (2000).
9. I. Timofeev, F. Grenier, M. Steriade, *Proc. Natl. Acad. Sci. U.S.A.* **98**, 1924 (2001).

10. I. Ulbert, E. Halgren, G. Heit, G. Karmos, *J. Neurosci. Methods* **106**, 69 (2001).
11. Materials and methods are available as supporting material on *Science* Online.
12. M. Massimini, R. Huber, F. Ferrarelli, S. Hill, G. Tononi, *J. Neurosci.* **24**, 6862 (2004).
13. J. Numminen, J. P. Makela, R. Hari, *Electroencephalogr. Clin. Neurophysiol.* **99**, 544 (1996).
14. M. Velasco *et al.*, *Clin. Neurophysiol.* **113**, 25 (2002).
15. R. A. Wennberg, A. M. Lozano, *Clin. Neurophysiol.* **114**, 1403 (2003).
16. M. Volgushev, S. Chauvette, M. Mukovski, I. Timofeev, *J. Neurosci.* **26**, 5665 (2006).
17. M. Mukovski, S. Chauvette, I. Timofeev, M. Volgushev, *Cereb. Cortex* **17**, 400 (2007).
18. F. Amzica, M. Steriade, *Neurology* **49**, 952 (1997).
19. M. Bazhenov, I. Timofeev, M. Steriade, T. J. Sejnowski, *J. Neurosci.* **22**, 8691 (2002).
20. A. Compte, M. V. Sanchez-Vives, D. A. McCormick, X. J. Wang, *J. Neurophysiol.* **89**, 2707 (2003).
21. M. O. Cunningham *et al.*, *Proc. Natl. Acad. Sci. U.S.A.* **103**, 5597 (2006).
22. D. Contreras, A. Destexhe, T. J. Sejnowski, M. Steriade, *Science* **274**, 771 (1996).
23. J. A. Hobson, E. F. Pace-Schott, *Nat. Rev. Neurosci.* **3**, 679 (2002).
24. R. Stickgold, *Nature* **437**, 1272 (2005).
25. G. Tononi, C. Cirelli, *Sleep Med. Rev.* **10**, 49 (2006).
26. S. Ribeiro *et al.*, *PLoS Biol.* **2**, E24 (2004).
27. A. Rechtschaffen, A. Kales, *A Manual of Standardized Terminology, Techniques and Scoring System for Sleep Stages of Human Subjects*. (U.S. Government Printing Office, Washington, DC, 1968).
28. Supported by National Institute of Neurogical Disorders and Stroke (NIH) grants NS18741 and NS44623 to E.H. and Neuroprobes IST-027017, OTKA49122, ETT135/2006, János Szentágothai Knowledge Center RET 05/2004 grants to I.U. We thank L. Papp for technical support; and L. Grand, A. Magony, B. Dombovári, and D. Fabó for support in data analysis and recording. The authors dedicate this work to the memory of Edward Bromfield, who passed away on 10 May 2009.

Supporting Online Material
www.sciencemag.org/cgi/content/full/324/5930/1084/DC1
Materials and Methods
Fig. S1
Table S1
References

11 December 2008; accepted 20 March 2009
10.1126/science.1169626

Crystal Structure of the Nuclear Export Receptor CRM1 in Complex with Snurportin1 and RanGTP

Thomas Monecke,[1]* Thomas Güttler,[2]* Piotr Neumann,[1] Achim Dickmanns,[1] Dirk Görlich,[2]† Ralf Ficner[1]

CRM1 mediates nuclear export of numerous unrelated cargoes, which may carry a short leucine-rich nuclear export signal or export signatures that include folded domains. How CRM1 recognizes such a variety of cargoes has been unknown up to this point. Here we present the crystal structure of the SPN1·CRM1·RanGTP export complex at 2.5 angstrom resolution (where SPN1 is snurportin1 and RanGTP is guanosine 5′ triphosphate–bound Ran). SPN1 is a nuclear import adapter for cytoplasmically assembled, m_3G-capped spliceosomal U snRNPs (small nuclear ribonucleoproteins). The structure shows how CRM1 can specifically return the cargo-free form of SPN1 to the cytoplasm. The extensive contact area includes five hydrophobic residues at the SPN1 amino terminus that dock into a hydrophobic cleft of CRM1, as well as numerous hydrophilic contacts of CRM1 to m_3G cap-binding domain and carboxyl-terminal residues of SPN1. The structure suggests that RanGTP promotes cargo-binding to CRM1 solely through long-range conformational changes in the exportin.

Nuclear transport proceeds through nuclear pore complexes (NPCs) and supplies cell nuclei with proteins and the cytoplasm with nuclear products such as ribosomes and tRNAs. Most nuclear transport pathways are mediated by importin β–type nuclear transport receptors, which include nuclear export receptors (exportins), as well as importins (*1*, *2*). These receptors bind cargoes directly or through adapter molecules, shuttle constantly between the nucleus and cytoplasm, and use the chemical potential of the nucleocytoplasmic RanGTP-gradient to act as unidirectional cargo pumps (where GTP is guanosine 5′ triphosphate and RanGTP is GTP-bound Ran) (*3*).

Exportins recruit cargo at high RanGTP levels in the nucleus, traverse NPCs as ternary cargo·exportin·RanGTP complexes, and release their cargo upon GTP hydrolysis into the cytoplasm. CRM1 (exportin1/Xpo1p) (*4*, *5*) and CAS (Cse1p/exportin2) (*6*) are the prototypical exportins. Whereas CAS is specialized to retrieve the nuclear import adapter importin α back to the cytoplasm (*6*), CRM1 exports a very broad range of substrates from nuclei (*4*, *5*, *7*–*11*), including ribosomes and many regulatory proteins. It also depletes translation factors from nuclei and is essential for the replication of viruses such as HIV.

CRM1 has a dual function during biogenesis of spliceosomal U small nuclear ribonucleoproteins (snRNPs). It exports m^7G-capped U small nuclear RNAs to the cytoplasm (*4*, *12*), where they recruit Sm-core proteins and receive a 2,2,7-trimethyl (m_3G) cap structure. The import adapter snurportin 1 (SPN1) and importin β then transport the mature m_3G-capped U snRNPs into nuclei (*13*). To mediate another import cycle, SPN1 is returned to the cytoplasm by CRM1 (*14*).

Many CRM1 cargoes harbor a leucine-rich nuclear export signal (NES) that typically includes four characteristically spaced hydrophobic residues (*7*). Examples are the HIV-Rev protein (*15*) or the protein kinase A inhibitor (PKI) (*16*). In other cases, however, CRM1 recognizes not just a short peptide, but instead a large portion of the export cargo; here, SPN1 is the prototypical example (*14*). CRM1 binds SPN1 tighter than other export substrates, apparently because CRM1 must displace the imported U snRNP from SPN1 before export may occur.

The cytoplasmic dissociation of CRM1 from SPN1 is essential for multi-round import of U snRNPs. Hydrolysis of the Ran-bound GTP alone is insufficient to fully disrupt the interaction (Fig. 1, A to C) (*14*), but importin β can displace CRM1 from SPN1 (Fig. 1A). Thus, either the binding sites of SPN1 for CRM1 and importin β overlap, or importin β forces SPN1 into a conformation that is incompatible with CRM1 binding.

Two functional domains in SPN1 have been described: (i) the m_3G cap-binding domain ($SPN^{97–300}$) (*17*) and (ii) the N-terminal importin β–binding (IBB) domain ($SPN1^{40–65}$) (*14*, *18*, *19*), which confers binding to and import by importin β (*20*). A multiple alignment of SPN1 from various species revealed another conserved region that precedes the IBB domain and includes the hydrophobic residues Leu^4, Leu^8, Phe^{12}, and Val^{14}. Mutating any of those residues to serine or deleting Met^1 strongly impaired the interaction with CRM1, in particular at higher salt concentrations (Fig. 1B and fig. S1). Even though the SPN1 N terminus (with its conserved hydrophobic residues) resembles a classical NES, there are clear differences: foremost that CRM1 binds the isolated SPN1 N terminus ($SPN1^{1–21}$) considerably weaker than, for instance, the PKI-NES (Fig. 1C). In the context of full-length SPN1, however, this difference is more than compensated by the contribution of the m_3G cap-binding domain to the CRM1 interaction.

We then assembled, purified, and crystallized an export complex containing full-length human $SPN1^{1–360}$, full-length mouse $CRM1^{1–1071}$, and GTP-$RanQ69L^{1–180}$, a C-terminally truncated and GTPase-deficient form of human Ran (*21*).

[1]Abteilung für Molekulare Strukturbiologie, Institut für Mikrobiologie und Genetik, GZMB, Georg-August-Universität Göttingen, Justus-von-Liebig-Weg 11, 37077 Göttingen, Germany. [2]Abteilung Zelluläre Logistik, Max-Planck-Institut für Biophysikalische Chemie, Am Fassberg 11, 37077 Göttingen, Germany.

*These authors contributed equally to this work.
†To whom correspondence should be addressed. E-mail: goerlich@mpibpc.mpg.de

www.sciencemag.org/cgi/content/full/324/5930/1084/DC1

Supporting Online Material for

The Human K-Complex Represents an Isolated Cortical Down-State

Sydney S. Cash,* Eric Halgren, Nima Dehghani, Andrea O. Rossetti, Thomas Thesen, ChunMao Wang, Orrin Devinsky, Ruben Kuzniecky, Werner Doyle, Joseph Madsen, Edward Bromfield, Loránd Erőss, Péter Halász, George Karmos, Richárd Csercsa, Lucia Wittner, István Ulbert

*To whom correspondence should be addressed. E-mail: scash@partners.org

Published 22 May 2009, *Science* **324**, 1084 (2009)
DOI: 10.1126/science.1169626

This PDF file includes

The Human K-Complex Represents an Isolated Cortical Down-State

Supporting Online Material

Materials and Methods

Subjects. Eight patients (15-48 years old; 4 female) with long-standing pharmaco-resistant complex partial seizures participated after fully informed consent according to NIH guidelines as monitored by the local Institutional Review Boards. Simultaneous scalp, macroelectrode and microelectrode cortical recordings during natural sleep were made over the course of clinical monitoring for spontaneous seizures. Subdural grid and strip clinical electrode arrays were placed in order to confirm the hypothesized seizure focus, and locate epileptogenic tissue in relation to essential cortex, thus directing surgical treatment. Patients were all right-handed, with intelligence and personality in the normal range (see table S1 for clinical characteristics of individual patients). The decision to implant, the electrode targets and the duration of implantation were made entirely on clinical grounds without reference to this experiment. The patients were informed that participation in the experiment would not alter their clinical treatment in any way, and that they may withdraw at any time without jeopardizing their clinical care.

Probes. Macro-electrode contacts were 3mm platinum discs spaced 10mm center-to-center, embedded in 8x8 grid arrays, linear 1x8 strips or some combination thereof. Linear microelectrode arrays were placed perpendicular to the cortical surface within the hypothesized epileptogenic zone, passing ~3mm from the pial surface to the white matter, and recording en passant from the different lamina of a cortical column. Laminar microarrays consisted of 24 individual 90%Pt-10%Ir contacts, each 40μm in diameter and spaced 150μm center-to-center (*S1*). Electrodes were located relative to cortical gyri using intraoperative photographs, as well as CTs and MRIs taken with the probes in place. The depths of the laminar contacts below the pial surface are fixed and known because the top

of the probe is a silastic sheet that adheres by surface tension to the cortical surface. In addition, laminar contacts in gray matter, white matter, and CSF have characteristic activity patterns, assisting in resolution of their entry and exit points. In 3 cases the relationship of the probe to cortical lamina was confirmed with post-resection histological examination (example shown in fig. S1). Scalp EEG, electro-oculogram (EOG) and submental electromyogram (EMG) electrodes were placed to permit sleep staging (see below).

Recordings. Recordings from grid and strip macro-electrode arrays were made using 128 channel clinical cable telemetry systems with sampling rates between 200 and 800 Hz and bandpass from 0.1 to 100-400 Hz. These recordings were referenced to intradural electrodes facing away from the cortex. Recordings from microelectrode arrays used custom amplifiers in a differential configuration from 23 pairs of successive contacts, at 2 kHz (16 bit) sampling rate for field potentials and 20 kHz (12 bit) for unit activity, and stored continuously with stimulus and timing markers permitting synchronization with grid and strip recordings. Recordings were not analyzed if a patient had a seizure in the recording session, or if the local cortex exhibited chronic slow waves, interictal spikes or other frankly abnormal activity.

Estimation of population trans-membrane current flows and unit activity in different cortical layers. Population trans-membrane current flows were estimated using current source density (CSD) analysis (*S2*), calculated as the second spatial derivative of field potentials (0.5-30Hz) after applying a 5-point Hamming filter (*S1*) or by using the inverse CSD (iCSD) method of Pettersen et al. (*S3*). CSD may be due to either active transmembrane currents, or passive returns distributed according to the geometry of the cell. Active currents may be due to neurotransmitter-gated channels in the postsynaptic membrane, or to voltage-gated channels and other intrinsic membrane currents (*S4*). CSD analysis assumes that conductivity is uniform and isotropic in the tissue immediately

surrounding the probe (*S5*). This assumption has been tested in the hippocampus where deviations from the homogeneous approximation are too small to influence the spatial distribution of sources and sinks (*S6*).Variable electrode spacing or potential amplification could produce spurious CSD signals but these effects were evaluated experimentally in our system and were less than 5% (*S1*). CSD analysis will miss transmembrane currents if they do not result in a net radial extracellular current, as might happen if they are produced by synapses on a spherically symmetrical dendritic domain. CSD will also fail to detect currents that flow over distances that are small relative to the spatial sampling density. Modeling and experimental measures indicate that the center-to-center contact spacing of 150μm used in the current study is adequate to sample laminar CSD in macaque primary visual cortex (*S7, S8*). The limiting factor was the dendritic domains of stellate cells in thalamorecipient layer IVc. Cortex is thicker in humans, and the sampled areas are not known to have a thin but important sublayer comparable to IVc. Nonetheless, it is likely that the CSD analysis reported here is relatively insensitive to synaptic activity on layer IV stellate cells. Finally, current sources or sinks can be missed if the laminar probe does not sample the entire cortical depth. Multi-Unit Activity (MUA), an estimate of population neuronal firing, was calculated in each cortical layer by rectifying high frequency activity (300-5000 Hz) and smoothing with a 50 Hz low-pass filter (*S1*).

Time and frequency domain analysis were initially performed using Neuroscan Edit 4.3 software with spectral content of the LFP and CSD data evaluated using custom MatLab routines based on the EEGLAB package (*S9*). This approach is based on either a shorttime Fourier transform or sinusoidal wavelet transform. Both methods were tried without significant differences. The frequency changes were also evaluated using custom designed C++ and MatLab software (*S10, S11*) in which individual trial event-related spectral power (iERSP) was calculated by convoluting the single trial signal $s_i(t)$ for each channel i with complex Morlet's wavelets. In all cases, the resulting time-

frequency plots of spectral power were normalized with respect to an appropriate baseline (-500 to -100 ms before the K-complex) for each frequency and plotted as z-scores. There were no significant differences between the methods.

Sleep staging and grapho-element identification followed standard criteria and was verified by qualified raters. Sleep staging relied on direct behavioral observation, surface EEG (between one and four scalp electrodes referenced to the mastoid), EOG and submental EMG. Spontaneous KC were identified as multiphasic waves during Stage 2 sleep with a significant surface negative and then surface positive potential occurring ~500 and 900 ms from the beginning of the waveform. Stage 2 sleep was identified by observation of the patient's sleeping behavior as well as the absence of rapid eye movements, occasional delta activity (<20%), KC and spindles (*S12*).We also evoked KC during stage 2 sleep with simple auditory tones presented randomly (30-40s intervals) at an intensity that was gradually increased so that more than half of the tones evoked KC without eliciting arousal.

Histology of the region directly surrounding the recording electrode was obtained in 3 of the 8 patients. Two of those examinations revealed normal cortical neurons and layer architecture despite the presence of a dysplastic lesion in some other region. Figure S1 shows a photomicrograph of the tissue adjacent to one of these electrodes (Patient G). The third showed evidence of mild dysplasia. Inspection of pre-operative MRIs in 4 of the remaining 5 patients failed to show any structural abnormality in the region near the implantation. The fifth patient showed possible dysplastic tissue in the region of the array. Identical results were found in the two patients with evidence of dysplasia near the recording array compared to the other patients. An additional (ninth) patient was recorded but their data was rejected from consideration due the presence of obvious epileptiform activity. Therefore, the preponderance of data suggests that our recordings were done in relatively normal neuronal tissue and are unlikely to reflect pathological processes secondary to epilepsy.

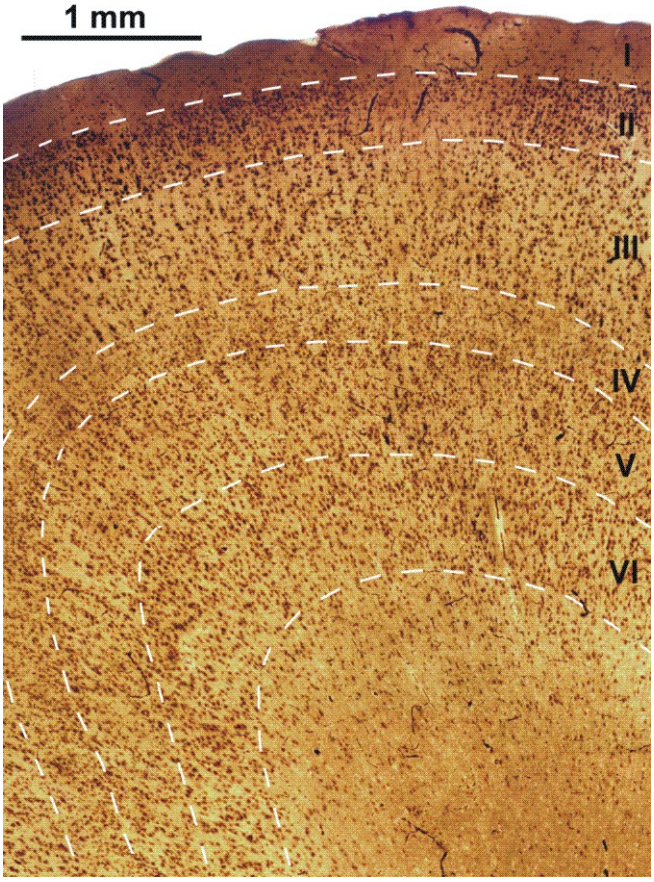

Fig. S1. Example histological exam of tissue immediately adjacent to the electrode tract in Patient G. Microphysiological recordings from this patient are shown in Fig. 3. The neuronal elements and laminar structure are grossly intact. 60-μm-thick section stained with NeuN.

Table S1: Patient characteristics.

Patient	**Gender**	**Age**	**Focus**	**Etiology**
A	M	15	Frontal	Dysplasia
B	F	27	Frontal	Unknown
C	M	39	Temporal	Dysplasia
D	M	16	Frontal	Dysplasia
E	F	18	Temporal	Dysplasia
F	F	48	Parietal	Dysplasia
G	M	35	Frontal	Dysplasia
H	F	34	Frontal	Dysplasia

References

S1. I. Ulbert, E. Halgren, G. Heit, G. Karmos, *Journal of Neuroscience Methods* **106**, 69 (2001).
S2. C. Nicholson, J. A. Freeman, *Journal of Neurophysiology* **38**, 356 (1975).
S3. K. H. Pettersen, A. Devor, I. Ulbert, A. M. Dale, G. T. Einevoll, *J Neurosci Methods* **154**, 116 (2006).
S4. S. Murakami, T. Zhang, A. Hirose, Y. C. Okada, *J Physiol* **544**, 237 (2002).
S5. U. Mitzdorf, *Physiol Rev* **65**, 37 (1985).
S6. J. Holsheimer, *Exp Brain Res* **67**, 402 (1987).
S7. C. Schroeder, A. Mehta, S. Givre, *Cereb Cortex* **8**, 575 (1998).
S8. C. E. Tenke, C. E. Schroeder, J. C. Arezzo, H. G. Vaughan, Jr., *Exp Brain Res* **94**, 183 (1993).
S9. A. Delorme, S. Makeig, *Journal of Neuroscience Methods* **134**, 9 (2004).
S10. E. Halgren, C. Boujon, J. Clarke, C. Wang, P. Chauvel, *Cerebral Cortex* **12**, 710 (2002).
S11. C. Wang, I. Ulbert, D. L. Schomer, K. Marinkovic, E. Halgren, *J Neurosci* **25**, 604 (2005).
S12. A. Rechtschaffen, A. Kales, *A manual of standardized terminology, techniques and scoring system for sleep stages of human subjects*. (US Government Printing Office, Washington,DC, 1968).